



# SIMULATION AND INVESTIGATION OF NANO-REFRIGERANT FLUID CHARACTERISTICS WITH THE TWO-PHASE FLOW IN MICROCHANNEL

Ammar Hassan Soheel, Omar Mahmood Jumaah, Ahmed Mustaffa Saleem\*

*Technical Engineering College, Northern Technical University, Mosul, 41001, Iraq*

## ABSTRACT

This paper presents a simulation and investigation of the heat transfer coefficient, pressure drop, and thermal conductivity of two - phase flow. The simulation was performed of mixtures ( $Al_2O_3$  nanoparticles with R134a refrigerant). The size of nanoparticles ( $Al_2O_3$ ) which is used in this study is 30 nm and volume concentrations are 0.015 and 0.03. The two – phase flowing through a horizontal circular microchannel of (diameter 100  $\mu m$ , and length 20 mm) under constant heat flux (3000  $W/m^2$ ) and constant wall temperature (330 K), also in this study used the inlet temperature at -20  $^{\circ}C$  and mass flow rates are 0.3, 0.4, 0.5, 0.6, 0.7 and 0.8 g/s using in the dissipation of heat from electronic circuits by evaporation. The simulation is achieved by CFD numerical model using FLUENT ANSYS version 15 software. The results indicate the best temperature, pressure drop, density and volume fraction for two-phase flow nanorefrigerant in the microchannel. The higher heat transfer coefficient and pressure drop of two-phase nanorefrigerant flow at a high volume concentration (0.03) of  $Al_2O_3$  when the mass flow rate is maximum. Finally, compared heat transfer coefficient of this study with the results of Kumar et al. (2013) at variation the mass flow rate, and found the root mean square of error (10%), also compared heat transfer coefficient of this study with results of Hernández et al. (2016) at variable volume concentration of nanoparticles  $Al_2O_3$ , and found the root mean square of error (3.7%).

**Keywords:** *Nanorefrigerant, Two-phase microchannel, R134a,  $Al_2O_3$  nanoparticles, Heat transfer Coefficient.*

## 1. INTRODUCTION

For engineers who work over decades to develop better heat transfer in various applications, nano-fluid has become an interesting topic. A Nanofluid is a new type of heat transfer fluid that operates in conventional host fluids with nanoparticles, enhances the surface contact area, nano-refrigerants are nanofluids and host fluids are coolant. The potential of R134a to deplete global warming (GWP) and ozone (ODP) is lower than that of other coolants Singh et al. (2015).  $Al_2O_3$  nanoparticles have the highest use in the cooling system, because they are not costly, easier to disperse and are not healthy and efficient in host refrigerants Patil et al. (2015). There has been more and more research in recent years on the two-phase flows of heat and fluid dynamics in microchannels. It is common knowledge that a higher heat transfer factor can be obtained at some mass velocity by reducing hydraulic diameter at the expense of greater frictional pressure drop, based on macro-scale convective heat transfer within the channels. Microchannels, for instance heat pipes, electronics and automotive condensers, are used in many different applications Cavallini et al. (2005).

The system assumes complex fluid behaviors when two phases are confined into a microchannel. The predominance of surface forces (surface tension etc.) causes the two-phase flow of gas fluid in the microchannels to compare itself with conventionally large-sized tubes (>10 mm) Yue et al. (2004) as the channel diameter decreases. The temperature of an electronic device increases fairly consistently with increasing heat flow for a certain thermal resistance sink and ambient temperature. For defense electronics, this relationship is particularly problematic Lee et al. (2009).

The two phase heat sinks of the microchannel are not without inconvenience. The small hydraulic diameter is likely to result in a significant drop in the pressure and a corresponding increase in the consumption of electronic systems, which is unwanted. For microchannel heat sink design, a strong understanding of the relationship between pressure drop and flux and heat flux is crucial Lee et al. (2005). Qu et al. (2003) dedicated to the measurement and prediction in water-cooled rectangular thermal dish heating of a saturated flow boiling thermal transfer coefficient. The model predictions and heat transmission coefficients over wide ranges of flux and heat flow were well agreed. Lee et al. (2004) investigated experimentally the two-phase pressure drop and the boiling coefficient of heat transfer R14a through the rectangular heat sink used to evaporate the cooling cycle. The study showed a general increase in the total pressure drop as mass speed and heat flux increase. And for both R134a and water it offers excellent predictions when a new coefficient of the heat transfer correlation was recommended. Cavallini et al. (2005) studied experimentally the lower pressure properties of R236ea, R134a and R410A multipoint mini-channel, adiabatic two-phase flow. The experimental findings indicate that the correlations provided can reasonably well forecast the gradient of R134a friction. However, R236ea and even worse data for R410A were not satisfactorily agreed. Fukagata et al. (2007) performed a two-phase air and water simulation in the microtube. They focused on the characteristics of flow and heat transfer in bladder train flow. Because the local temperature differences were slight, the Nusselt number was huge beneath the bubble and the heat transfer was also increased by the liquid tension because of the circulating stream. Yang et al. (2008) investigated the boiling of R141B flow in a horizontal rolling tube. It had been discovered that a significant impact of the phase distribution on the two-phase temperature profile and

\* Corresponding author. Email: [ahmedmustafa@ntu.edu.iq](mailto:ahmedmustafa@ntu.edu.iq)

that greater temperatures always appear in the vapor region. Lee et al. (2009) explored the advantages of direct cooling systems cooling the device. In a conventional vapor compression cycle, R134a acts as a work fluid, using a rectangular microchannel heat sink. The thermodynamic balance quality of the convective heat transfer coefficient was highest close to zero. Hanafizadeh et al. (2011) studied experimentally vertical mini pipes air-water two-phase flow regimes. Different air-water flow patterns in the small tube at different air and water flow rates were observed at the same time. Zhao et al. (2013) investigated the pressures of gas-liquid two phases within rectangular T-junction microchannels handled on the hydrodynamic characteristics. At atmospheric and high pressure respectively, 7 typical flow patterns were observed. Kumar et al. (2013) described the R134a two-phase fluid flow in a circular microchannel by present a CFD model for void fraction, pressure drop, and heat transfer coefficient. The result was a high reduction in the pressure at a very low mass flow rate, and the thermal transfer coefficient increases as the mass flow rate increases. Cho et al. (2014) investigated numerically and experimentally of two-phase in a rectangular microchannel with heterogeneous surface. The hard surface had been affected two-phase circulation. Autee et al. (2016) studied experimentally of two-phase drop in flow pressure in small bends in diameter. In curvature multiplier to two phase pressure drops developed a new correlation. Bartkus et al. (2017) investigated experimentally two phases of a rectangular microchannel with T- mixture of ethanol nitrogen mixture gas-liquid flow. They observed the maps of microchannel flow regimes. Le et al. (2018) examined the effect on the transition phase between liquid and vapor of the rounded edge rectangular microchannel geometry numerically and experimentally for two phased flow. The outlet temperature and vapor quality of rectangular heat sinks at the rounded edge were found. Lewis et al. (2018) studied the pressure loss in a rectangular microchannel associated with the two-phase flow suddenly expanded into a multiplex in experiment. Ravangard et al. (2019) developed numerically modeling two-phase in a microchannel that was compatible with high density ratio. A qualitative flow criterion had been presented in a particular geometry microchannel. Pamitran et al. (2020) studied the temperature and heat measurement characteristics in a circular microchannel for a double-phase flow boiling R-290. The surface temperature increased with the test section, and heat transfer from the boiling of two-phase flow nucleate in a microchannel is affected by boiling the core heat transfer nucleates and was slightly affected by convective heat transfer. Nair et al. (2020) presented the analysis of numerical heat transfer and the quantification for the pressure drop by the flooded evaporator chiller  $Al_2O_3 - R718$ -based nanorefrigerant flow. R718 (water) was one of the secondary coolants most commonly used in HVAC applications. Kumar et al. (2020) investigated exergy analysis of nanofluid flow through heat exchanger channels. The net impact of relative variations in the thermophysical properties of the nanoparticles, which were sensitive to numerous parameters including size and shape, material and concentration, as well as based fluid thermal properties, was used to determine the improvement of exergy efficiency of nanofluid flow through heat exchanger. Al-Zaidi et al. (2021) studied experimentally the effect of HFE-7100 channel aspect ratio in copper multi-micro-channel heat sinks on flow-boiling characteristics (flow patterns, thermal transfer and pressure drop). Three heat sinks with 500mm<sup>2</sup> base area, a hydraulic channel diameter of 0.46mm and a channel aspect ratio of 0.5, 1.0 and 2.0 had been tested.

The aim of this paper, however, is to analyze and simulate the coefficient of heat transfer, pressure drop and thermal conduct of two phase (liquid & solid) fluid flow in a Microchannel using ANSYS FLUENT version 15 software to analyze the defense electronics CFD thermal transfer.

## 2. COMPUTATIONAL PROGRAMME

### 2.1 Physical Model

Considering a copper smooth horizontal micro tube of an evaporator inner diameter "100  $\mu\text{m}$ ", and length "20 mm" is shown in Fig. 1. The nanoparticles  $Al_2O_3$  (30 nm) mixes with refrigerant (R134a) at constant inlet temperature ( $T_{in}$ ) and mass flow rate ( $\dot{m}_{in}$ ) flows through microtube under constant heat flux ( $q''_w$ ).

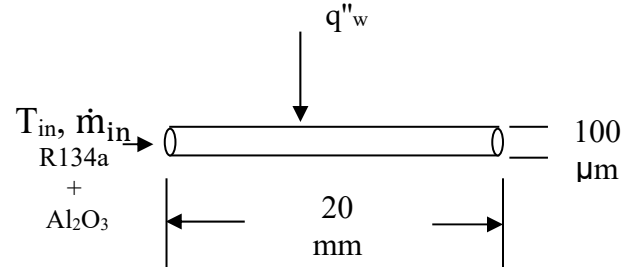


Fig. 1 Schematic of the microtube.

### 2.2 Meshing

The horizontal microtube is designed, meshing and simulated using FLUENT ANSYS version 15 software, as shown in Fig. 2.

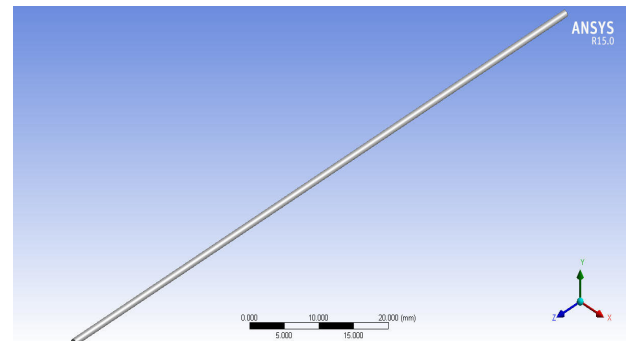


Fig. 2 The geometric of the horizontal microtube.

The grid independence test is performed to ensure the accuracy of the numerical results. A series of grid addition tests were performed to ensure that the computer mesh was optimized.

For each element of a model, a quality factor is calculated (excluding line and point elements). The Quality Element Option offers a composite metric ranging from 0 to 1. The ratio of volume to edge length for a given element is based on this measurement. A value of 1 indicates a perfect cube or square, while 0 indicates a zero or negative volume of the component Soheel et al. (2018).

The mesh of independence of 253635 element number and element quality in this study as shown in Fig. 3 and Fig. 4 is 0.908558711, and as shown in Table 1.

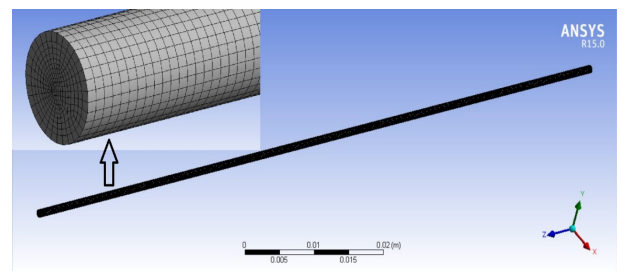


Fig. 3 The configuration meshes of the horizontal microtube.

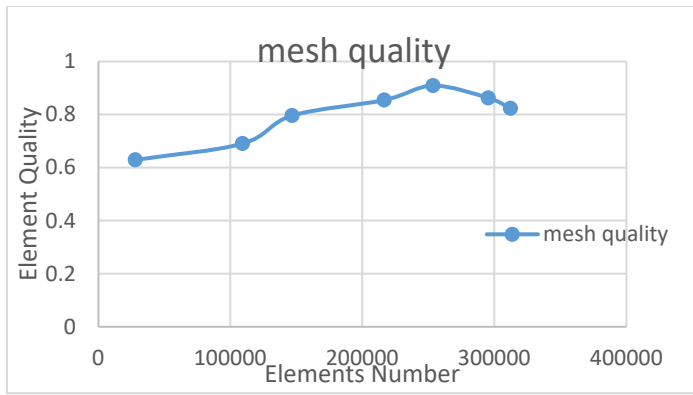


Fig. 4 Mesh quality (stability of mesh).

Table 1 Element quality.

Element Quality	Elements Number
0.629268976	28028
0.690200825	109252
0.795995261	146786
0.854734954	216584
0.908558711	253635 (Best Mesh)
0.86245279	295415
0.823070669	312220

### 3. MATHEMATICAL MODEL

To obtain the heat transfer coefficient, pressure drop, and thermal conductivity, of nanorefrigerant two-phase flow in a microchannel, the mixture and (k-ε) turbulent model were employed and calculated their properties in mixture flow application Hernández et al. (2016). The steps fluctuate at different speeds according to the sliding speed concept. For the pressure-velocity connection a SIMPLE algorithm has been chosen, solved all phase velocity correction and pressures correction equations. The flow was steady-state, compressible and three dimensional. The resistance conduction around the microtube was negligible.

The mixture's continuity equation as the following:

$$\frac{\partial}{\partial t}(\rho_m) + \nabla(\rho_m \vec{v}_m) = 0 \quad (1)$$

Average speed flow can be calculated as the following:

$$\vec{v}_m = \frac{\sum_{k=1}^n \varphi_k \rho_k \vec{v}_k}{\rho_m} \quad (2)$$

The density of the mixture is defined as the following equation:

$$\rho_m = \sum_{k=1}^n \varphi_k \rho_k \quad (3)$$

The mixture momentum equation is obtained by adding dynamic equations for each phase as the following:

$$\frac{\partial}{\partial t}(\rho_m \vec{v}_m) + \nabla(\rho_m \vec{v}_m \vec{v}_m) = -\nabla p + \nabla \left[ \mu_m (\nabla \vec{v}_m + \nabla \vec{v}_m^T) \right] \dots + \rho_m \vec{g} + \vec{F} + \nabla \left( \sum_{k=1}^n \varphi_k \rho_k \vec{v}_{dr,k} \vec{v}_{dr,k} \right) \quad (4)$$

The mixture viscosity is defined by the following equation:

$$\mu_m = \sum_{k=1}^n \varphi_k \mu_k \quad (5)$$

The drift velocity of the second phase is determined as the following:

$$\vec{v}_{dr,k} = \vec{v}_k - \vec{v}_m \quad (6)$$

The energy equation is determined from the following equation:

$$\frac{\partial}{\partial t} \sum_{k=1}^n (\varphi_k \rho_k E_k) + \nabla \sum_{k=1}^n (\varphi_k \vec{v}_k (\rho_k E_k + p)) = \dots \nabla (K_{eff} \nabla T) + S_E \quad (7)$$

The effective thermal conductivity is expressed as the following:

$$K_{eff} = \sum \varphi_k (K_k + K_t) \quad (8)$$

The volume fraction equation of the second phase can be obtained from the continuity equation:

$$\frac{\partial}{\partial t} (\varphi_p \rho_p) + \nabla (\varphi_p \rho_p \vec{v}_p) = -\nabla (\varphi_p \rho_p \vec{v}_{dr,p}) \dots + \sum_{q=1}^n \dot{m}_{qp} - \dot{m}_{pq} \quad (9)$$

Thermo physical properties of the Al<sub>2</sub>O<sub>3</sub> nanoparticles are specified in Table 2. These properties are adopted from Zawawi et al. (2017).

Table 2 Thermo physical properties of Al<sub>2</sub>O<sub>3</sub> nanoparticles.

Properties	Value
Density (kg/m <sup>3</sup> )	4000
Specific Heat (J/kg.K)	773
Thermal Conductivity (W/m.K)	36

Table 3 illustrates the thermo physical properties of R134a. These properties are adopted from ASHRAE Handbooks (2009).

Table 3 Thermo physical properties of R134a.

Properties	Unit	Value
Pressure	MPa	0.13273
Density (Liquid)	kg/m <sup>3</sup>	1358.3
Dynamic viscosity (Liquid)	Pa.s	0.000353
Dynamic viscosity (Vapour)	Pa.s	0.00000992
Thermal Conductivity (Liquid)	W/m.K	0.1011
Thermal Conductivity (Vapour)	W/m.K	0.00982

### 4. RESULTS AND DISCUSSION

This study simulates heat transfer coefficient, pressure drop, thermal conductivity, volume fraction, temperature distribution, and density of mixture two-phase flow (Al<sub>2</sub>O<sub>3</sub> with R134a) through microchannel. This study selected two volume concentration of nanoparticles dispersed in the refrigerant of 0.015 and 0.03 with a masses flow rate of 0.3,0.4,0.5,0.6,0.7 and 0.8 g/s, at constant heat flux (3000 W/m<sup>2</sup> and inlet nanorefrigerant temperature 253 K were used in this

study. The results are simulated in the CFD technique applied with FLUENT ANSYS 15 software.

The temperature contours of nanorefrigerant two-phase flows in a horizontal microtube are shown in Fig. 5. It can be observed that the behaviour of temperatures for nanorefrigerant and increasing it's along the microchannel due to evaporation. These increases in temperatures are due to the interface of liquid – gas of refrigerants through evaporation.

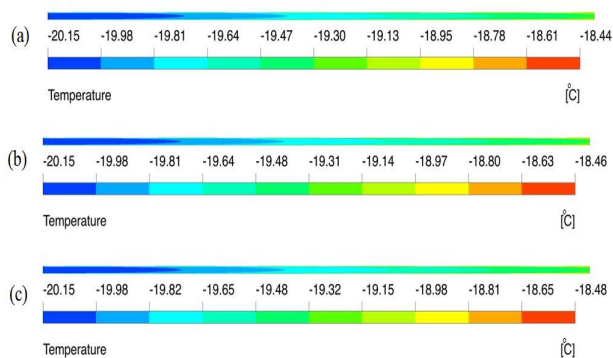


**Fig. 5** Temperatures contours of the two-phase flows nanorefrigerant at heat flux  $3000 \text{ W/m}^2$  and mass flow rate  $0.4 \text{ g/s}$ . (a) R134a, (b) R134a with  $0.015$  of  $\text{Al}_2\text{O}_3$ , (c) R134a with  $0.03$  of  $\text{Al}_2\text{O}_3$ .

Fig. 6 represents pressure drop through the microtube of mixture ( $\text{Al}_2\text{O}_3$  with R134a) for (a) pure R134a, (b)  $\text{Al}_2\text{O}_3$  at volume concentration ( $0.015$ ) with R134a, and (c)  $\text{Al}_2\text{O}_3$  at volume concentration ( $0.03$ ) with R134a. Fig. 6 indicates the maximum value of pressure drop occurs at volume concentration ( $0.03$ ) of  $\text{Al}_2\text{O}_3$ .

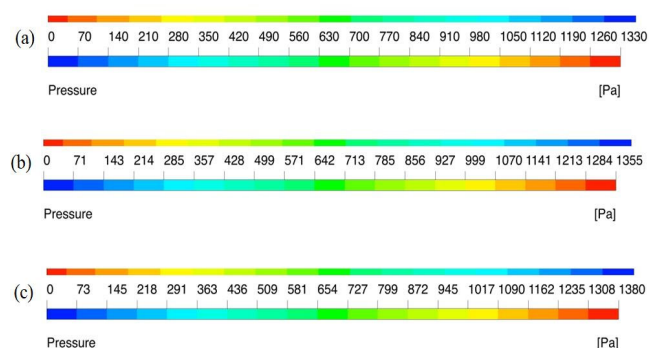
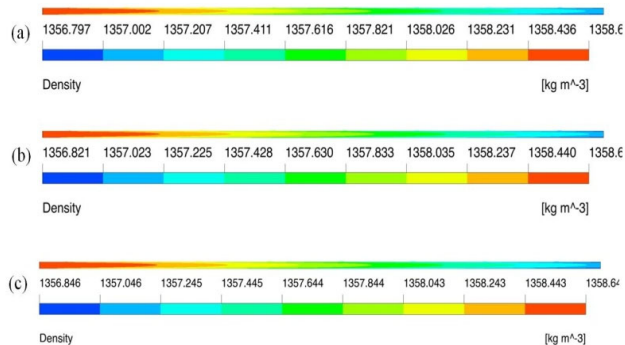


**Fig. 6** Pressure drop contours of the of the two-phase flow nanorefrigerant at constant heat flux  $3000 \text{ W/m}^2$  and mass flow rate  $0.5 \text{ g/s}$ . (a) R134a, (b) R134a with  $0.015 \text{ Al}_2\text{O}_3$ , (c) R134a with  $0.03 \text{ Al}_2\text{O}_3$ .

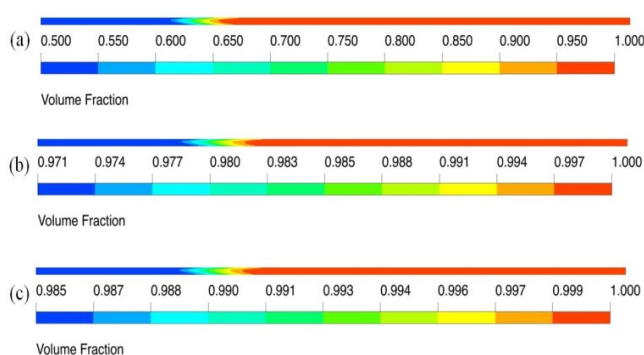
The behaviour of nanorefrigerant density along the microtube illustrates in Fig.7. It can be observed from this figure that the density of nanorefrigerant drops slowly along the tube due to increased temperature.

The volume fraction of the refrigerant distributed along the microchannel increases towards the outlet due to the introduction of the dispersed turbulence physics, as shown in Fig. 8.

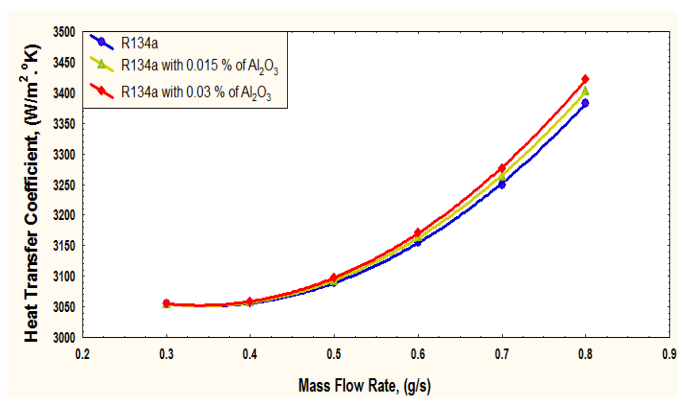
When the mass flow rate increases with the increases volume concentration of  $\text{Al}_2\text{O}_3$  nanoparticles, the heat transference coefficient of the two - phases flow of the nanoparticles increases, as shown in Fig. 9. Increases of heat transference coefficient are due to the increases thermal conductivity and surface area in refrigerants of  $\text{Al}_2\text{O}_3$  nanoparticles. Also Fig. 9 illustrates the influence of the volume concentration of  $\text{Al}_2\text{O}_3$  nanoparticles on the heat transfer ratio in the microtube at a continuous heat flux of  $3000 \text{ W/m}^2$  and the mass flow rate of the two-phase nanoparticles.



**Fig. 7** Density contours of the of the two-phase flows nanorefrigerant at heat flux  $3000 \text{ W/m}^2$  and mass flow rate  $0.7 \text{ g/s}$ . (a) R134a (b), R134a with  $0.015$  of  $\text{Al}_2\text{O}_3$ , (c) R134a with  $0.03$  of  $\text{Al}_2\text{O}_3$ .



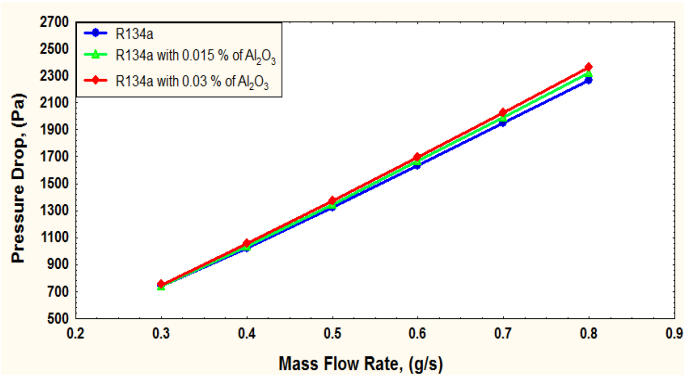
**Fig. 8** Volume fraction contours of the two-phase flows nanorefrigerant at heat flux  $3000 \text{ W/m}^2$  and mass flow rate  $0.6 \text{ g/s}$ . (a) R134a, (b) R134a with  $0.015$  of  $\text{Al}_2\text{O}_3$ , (c) R134a with  $0.03$  of  $\text{Al}_2\text{O}_3$ .



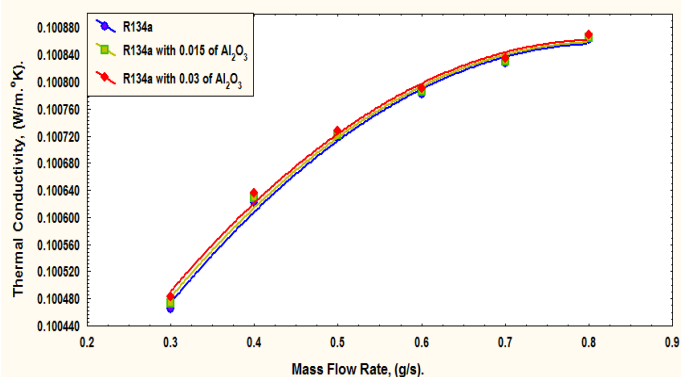
**Fig.9** Heat transfer coefficient of two-phase flow nanorefrigerant for pure R134a, ( $0.015$ )  $\text{Al}_2\text{O}_3$  with R134a and ( $0.03$ )  $\text{Al}_2\text{O}_3$  with R134a at constant heat flux ( $3000 \text{ W/m}^2$ ).

Fig. 10 shows the effect of the volume concentration of  $\text{Al}_2\text{O}_3$  nanoparticles which mixes with refrigerant R134a on the pressure drops of flow with variety of mass flow rates through a microtube at heat flux is  $3000 \text{ W/m}^2$ . Also this figure illustrates the pressure drops of two – phase flow are linearly incrementally.

Fig. 11 presents thermal conductivity with variation of mass flow rates of mixtute ( $\text{Al}_2\text{O}_3$  nanoparticles with refrigerant R134a). This figure shows that thermal conductivity increases with increases mass flow rates of mixtute ( $\text{Al}_2\text{O}_3$  nanoparticles at volume concentration ( $0.015$ ) and ( $0.03$ ) with refrigerant R134a), and has a major impact at  $0.8 \text{ g/s}$  mass flow when nanorefrigerant mixes with  $\text{Al}_2\text{O}_3$  nanoparticles at  $0.03$  volume concentration with heat flux ( $3000 \text{ W/m}^2$ ).



**Fig. 10** Pressure drop of two-phase flow nanorefrigerant for pure R134a, (0.015) Al<sub>2</sub>O<sub>3</sub> with R134a and (0.03) Al<sub>2</sub>O<sub>3</sub> with R134a at constant heat flux (3000 W/m<sup>2</sup>).

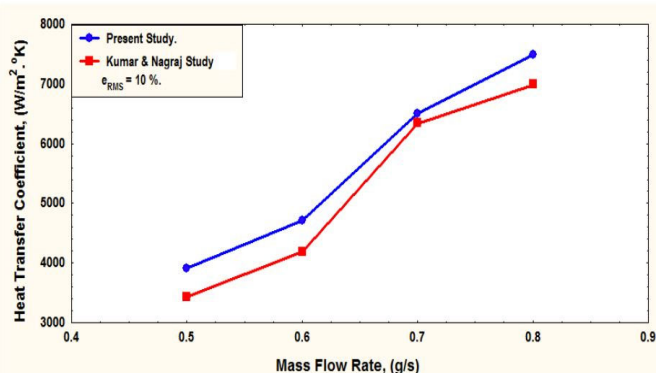


**Fig. 11** Thermal conductivity of two-phase flow nanorefrigerant for pure R134a, (0.015) Al<sub>2</sub>O<sub>3</sub> with R134a and (0.03) Al<sub>2</sub>O<sub>3</sub> with R134a at constant heat flux (3000 W/m<sup>2</sup>).

## 5. VALIDATION OF RESULTS

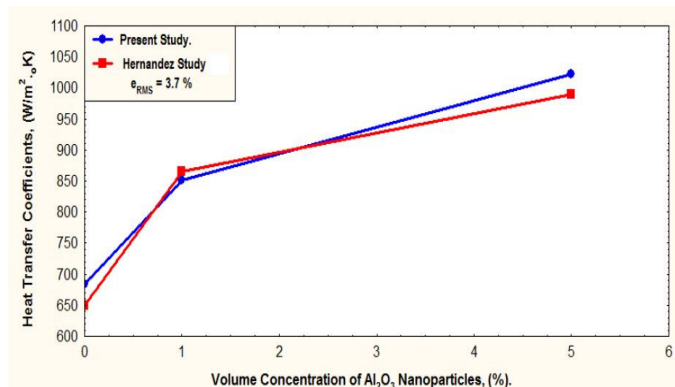
A comparison between this model with previous results studies of Kumar et al. (2013) and Hernández et al. (2016), as shown in Fig. 12 and Fig. 13, respectively, is carried out to validate the results of a model program which represents simulating and investigating heat transfer coefficient in a horizontal microchannel for the two-phase flow nanorefrigerant.

Fig. 12 illustrates the comparison results of heat transfer coefficient of present study with results of Kumar et al. (2013) at variation of mass flow rates of mixture (Al<sub>2</sub>O<sub>3</sub> nanoparticles and refrigerant R134a) coolant flow through the microchannel at constant heat flux flow (3000W/m<sup>2</sup>).



**Fig. 12** Comparison of heat transfer coefficient of the present results with results of Kumar et al. (2013).

Fig. 13 represents the comparison of heat transfer coefficient of present results with results of Hernández et al. (2016) at variation of volume concentration of Al<sub>2</sub>O<sub>3</sub> nanoparticles mixed with refrigerant R134a coolant flow through the microchannel at constant wall temperature (330 K).



**Fig. 13** Comparison of heat transfer coefficients of present results with results of Hernández et al. (2016).

## 6. CONCLUSIONS

The numerical model is used to simulate the effect of volume concentration of Al<sub>2</sub>O<sub>3</sub> nanoparticles mixed with refrigerants R134a, on the heat transfer coefficient, pressure drop, and thermal conductivity of flow through the microchannel, from the results, we can conclude the following:

1. The best temperature, pressure drop, density, and volume fraction for two-phase nanorefrigerant flow through the microchannel from the model are obtained.
2. When a maximum mass flow rate of two-phase nanorefrigerant is reached in the microchannel, a higher heat transfer coefficient is achieved at a high volume concentration of (0.03) Al<sub>2</sub>O<sub>3</sub>.
3. The two-phase pressure drop presents linearly increment with a mass flow rate of nanorefrigerant incrementally when the volume concentration of Al<sub>2</sub>O<sub>3</sub> nanoparticles in the R134a refrigerant increment through the microchannel.
4. The thermal conductivity of two-phase nanorefrigerant flow is improved due to increased volume concentration of nanoparticles Al<sub>2</sub>O<sub>3</sub> boosting the best performance.
5.  $\epsilon_{RMS}$  is 10% for the comparison of the present results with Kumar et al. (2013) results of heat transfer coefficient for the two-phase R134a refrigerant at constant heat flux (3000 W/m<sup>2</sup>) through microchannels.
6. Also,  $\epsilon_{RMS}$  is 3.7% for comparison of the present results with Hernández et al. (2016), results of heat transfer coefficient at constant wall temperature (330 K) through a microchannel at the variation of volume concentration of Al<sub>2</sub>O<sub>3</sub> nanoparticles mixed with refrigerant R134a.

## NOMENCLATURE

$E$	energy (W)
$e$	error
$g$	gravity acceleration (m/s <sup>2</sup> )
$K$	thermal conductivity (W/m.K)
$k$	turbulent fluctuation kinetic energy (m <sup>2</sup> /s <sup>2</sup> )
$\dot{m}$	mass flow of refrigerant (kg/s)
$N$	several phases
$P$	pressure drop of nanorefrigerant (Pa)
$q''$	heat flux (W/m <sup>2</sup> )
$S_E$	volumetric heat sources (W)

$T$  temperature of nanorefrigerant (K)  
 $t$  time (s)  
 $v$  velocity

#### Greek Symbols

$\rho$  density (kg/m<sup>3</sup>)  
 $\phi$  volume fraction  
 $\mu$  dynamic viscosity (Pa.s)

#### Superscripts

$dr$  drift  
 $eff$  effective  
 $m$  inlet of the microchannel  
 $k$  phase of the mixture  
 $M$  mixture  
 $P$  phase of the mixture  
 $q$  phase of the mixture  
 $RMS$  root mean square  
 $t$  turbulent

## REFERENCES

- Al-Zaidi, A.H., Mahmoud, M.M., Karayiannis, T.G., 2021, "Effect of aspect ratio on flow boiling characteristics in microchannels", *International Journal of Heat and Mass Transfer*, 164, 1 – 18.  
<http://dx.doi.org/10.1016/j.ijheatmasstransfer.2020.120587>
- Autee, A.T., Giri, S.V., 2016, "Experimental study on two-phase flow pressure drop in small diameter bend," *Perspect. Sci.*, 8, 621–625.  
<http://dx.doi.org/10.1016/j.pisc.2016.06.038>
- Bartkus, G., Kozulin, I., Kuznetsov, V., 2017, "Experimental investigation of two-phase gas-liquid flow in a microchannel with T-junction," *EPJ Web Conf.*, 159, 1–4.  
<http://dx.doi.org/10.1051/epiconf/201715900004>
- Cavallini, A., Col, D.D., Doretti, L., Matkovi, M., Rosseto, L., Zilio, C., 2005, "Two-phase frictional pressure gradient of R236ea, R134a and R410A inside multiport mini-channels," *Exp. Therm. Fluid Sci.*, 29(7), 861–870.  
<http://dx.doi.org/10.1016/j.expthermflusci.2005.03.012>
- Cho, S.C., Wang, Y., 2014, "Two-phase flow dynamics in a microchannel with heterogeneous surfaces," *Int. J. Heat Mass Transf.*, 71, 349–360.  
<http://dx.doi.org/10.1016/j.ijheatmasstransfer.2013.12.023>
- Fukagata, K., Kasagi, N., Ua-arayaporn, P., Himeno, T., 2007, "Numerical simulation of gas-liquid two-phase flow and convective heat transfer in a microtube," *Int. J. Heat Fluid Flow*, 28(1), 72–82.  
<http://dx.doi.org/10.1016/j.ijheatfluidflow.2006.04.010>
- Hanafizadeh, P., Saidi, M.H., Gheimass, A.N., Ghanbarzadeh, S., 2011, "Experimental investigation of air-water, two-phase flow regimes in vertical mini pipe," *Sci. Iran.*, 18(4), 923–929.  
<http://dx.doi.org/10.1016/j.scient.2011.07.003>
- Hernández, D.C., Londono, C.N., Benabithé, Z.Z., 2016, "Analysis of working nanofluids for a refrigeration system", *DYNA*, 83(196), 176-183.  
<http://dx.doi.org/10.15446/dyna.v83n196.50897>
- Kumar, A., Sharma, L., Kumar, S., Thakur, R., Goel, B., Suri, A.R.S., Thapa, S., Kumar, N., Maithani, R., 2020, "A REVIEW ON EXERGY ANALYSIS OF NANOFLUID FLOW THROUGH SEVERAL CONDUITS", *Frontiers in Heat and Mass Transfer*, 14(30), 1-15.  
<http://dx.doi.org/10.5098/hmt.14.30>
- Kumar, P., Nagraj, M.R., 2013, "CFD Analysis of Fluid Flow and Heat Transfer in Two-Phase Flow Microchannels", *Int. J. Eng. Res. Technol.*, 2(8), 2132–2143.
- Le, B., Nguyen, V., Dang, T., 2018, "The Effects of Microchannel Geometry on Phase Transition for Two-Phase Flow in Microchannel Heat Sinks," *Int. J. Power Energy Res.*, 2(1), 16–24.  
<http://dx.doi.org/10.22606/ijper.2018.21002>
- Lee, J., Mudawar, I., 2004, "Two-phase flow in high-heat-flux micro-channel heat sink for refrigeration cooling applications: Part II - Heat transfer characteristics," *Int. J. Heat Mass Transf.*, 48(5), 941–955.  
<http://dx.doi.org/10.1016/j.ijheatmasstransfer.2004.09.019>
- Lee, J., Mudawar, I., 2005, "Two-phase flow in high-heat-flux micro-channel heat sink for refrigeration cooling applications: Part I - Pressure drop characteristics," *Int. J. Heat Mass Transf.*, 48(5), 928–940.  
<http://dx.doi.org/10.1016/j.ijheatmasstransfer.2004.09.018>
- Lee, J., Mudawar, I., 2009, "Low-temperature two-phase microchannel cooling for high-heat-flux thermal management of defence electronics," *IEEE Trans. Components Package. Technol.*, 32(2), 453–465.  
<http://dx.doi.org/10.1109/TCAPT.2008.2005783>
- Lewis, J.M., Wang, Y., 2018, "Investigating the pressure loss associated with two-phase flow in a rectangular microchannel suddenly expanding into a manifold," *Int. J. Hydrogen Energy*, 43(36), 17444–17460.  
<http://dx.doi.org/10.1016/j.ijhydene.2018.07.112>
- Nair, V., Parekh, A.D., Tailor, P.R., 2020, "Performance analysis of Al<sub>2</sub>O<sub>3</sub>- R718 nanorefrigerant turbulent flow through a flooded chiller tube: a numerical investigation", *Journal of the Brazilian Society of Mechanical Sciences and Engineering*, 4, 1–16.  
<http://dx.doi.org/10.1007/s40430-020-02429-9>
- Pamitran, A.S., Novianto, S., Gazali, N.M., Koestoer, R.A., 2020, "Flow Pattern of Two-phase Flow Boiling with Heat Transfer and Pressure Drop Using Natural Refrigerant (Propane) in Microchannel", *Journal of Novel Carbon Resource Sciences & Green Asia Strategy*, 7(4), 544 – 548.  
<https://dx.doi.org/10.5109/4150474>
- Patil, M.S., Kim, S.C., See, J.H., Lee, M.Y., 2015, "Review of the Thermo-Physical Properties and Performance Characteristics of a Refrigeration System Using Refrigerant-Based Nanofluids", *energies*, 9(22), 1 – 16.  
<http://dx.doi.org/10.3390/en9010022>
- Qu, W., Mudawar, I., 2003, "Flow boiling heat transfer in two-phase microchannel heat sinks - II. Annular two-phase flow model," *Int. J. Heat Mass Transf.*, 46(15), 2773–2784.  
[http://dx.doi.org/10.1016/S0017-9310\(03\)00042-5](http://dx.doi.org/10.1016/S0017-9310(03)00042-5)
- Ravangard, A.R., Momayez, L., Rashidi, M., 2019, "Effects of geometry on simulation of two-phase flow in a microchannel with density and viscosity contrast," *J. Therm. Anal. Calorim.*, 139(1), 427–440.  
<http://dx.doi.org/10.1007/s10973-019-08342-1>
- Resources, R.C., 2009, "Thermophysical properties of refrigerants," *ASHRAE Handbooks – Fundamentals(SI)*, Chapter:30, 718, 1 - 30.
- Singh, S., Sharma, K., Lal, K., Tripathi, N.M., 2015, "To Study the Behaviour of Nanorefrigerant in Vapour Compression Cycle- a Review," *Int. J. Res. Eng. Technol.*, 4(4), 648–652.  
<http://dx.doi.org/10.15623/ijret.2015.0404111>

Kumar, P., Nagraj, M.R., 2013, "CFD Analysis of Fluid Flow and Heat

Soheel, A.H. et al.,2018, "Numerical investigation and comparison for heat transfer coefficient for two eco-friendly Nano refrigerants in horizontal tube," *international J. Eng. Technol.*, 7(4), 4949–4953.  
<http://dx.doi.org/10.14419/ijet.v7i4.19534>

Yang, Z. Peng, X.F., Ye, P.,2008, "Numerical and experimental investigation of two-phase flow during boiling in a coiled tube," *Int. J. Heat Mass Transf.*, 51(5 – 6), 1003–1016.  
<http://dx.doi.org/10.1016/j.ijheatmasstransfer.2007.05.025>

Yue, J., Chen, G., Yuan, Q., 2004, "Pressure drops of single and two-phase flows through T-type microchannel mixers," *Chem. Eng. J.*,

102(1), 11–24.

<http://dx.doi.org/10.1016/j.ccej.2004.02.001>

Zawawi, N.N.M., Azmi, W.H., Redhwan, A.A.M., Sharif, M.Z., Sharma, K.V., 2017," Thermo-physical properties of Al<sub>2</sub>O<sub>3</sub>-SiO<sub>2</sub>/PAG composite nanolubricant for refrigeration system", 80, 1 – 10.

<http://dx.doi.org/10.1016/j.ijrefrig.2017.04.024>

Zhao, Y., Chen, G., Ye, C., Yuan, Q.,2013, "Gas-liquid two-phase flow in the microchannel at elevated pressure," *Chem. Eng. Sci.*, 87(14), 122–132.

<http://dx.doi.org/10.1016/j.ces.2012.10.011>